

Environmental Controls on Diffusive and Ebullitive Methane Emission at a Sub-Daily Time Scale in the Littoral Zone of a Mid-Latitude Shallow Lake

Tsukuru Taoka¹, Hiroki Iwata¹, Ryuichi Hirata², Yoshiyuki Takahashi³, Yuichi Miyabara⁴, and Masayuki Itoh⁵

¹Shinshu University

²National Institute for Environmental Studies

³National Institute for Environmental studies

⁴Institute of Mountain Science, Shinshu University

⁵University of Hyogo

November 21, 2022

Abstract

Environmental controls on methane (CH) emission from lakes are poorly understood at sub-daily time scales due to a lack of continuous data, especially for ebullition. We used a novel technique to partition eddy covariance CH flux observed in the littoral zone of a mid-latitude shallow lake in Japan and examined the environmental controls on diffusion and ebullitive CH flux separately at a sub-daily time scale during different seasons. Both diffusive and ebullitive flux were significantly higher in summer than winter. The contribution of ebullitive flux to total flux was 56% on average. Diffusive flux increased with increasing wind speed due to increased subsurface turbulence. For a given wind speed, diffusive flux was higher in summer than in winter due to the higher concentration of dissolved CH in the surface water during summer. The transfer of accumulated dissolved CH from the bottom layer to the surface in summer and the accumulation of dissolved CH under surface ice in winter were important for explaining the variability of diffusive flux. In summer, ebullition tended to occur following triggers such as a decrease in hydrostatic pressure or an increase in wind speed. In winter, on the other hand, the impact of triggers was not obvious, and ebullition tended to occur in the morning when the wind speed began to increase. The low CH production rate in winter slowed the replenishment of bubbles in the sediment, negating the effect of triggers on ebullition.

1 **Environmental Controls on Diffusive and Ebullitive Methane Emission at a Sub-**
2 **Daily Time Scale in the Littoral Zone of a Mid-Latitude Shallow Lake**

3
4 **T. Taoka¹, H. Iwata¹, R. Hirata², Y. Takahashi², Y. Miyabara³, and M. Itoh⁴**

5 ¹Department of Environmental Science, Faculty of Science, Shinshu University, Matsumoto,
6 Japan.

7 ²Center for Global Environmental Research, National Institute for Environmental Studies,
8 Tsukuba, Japan.

9 ³Education and Research Center for Inland Water and Highland Environments, Faculty of
10 Science, Shinshu University, Matsumoto, Japan.

11 ⁴School of Human Science and Environment, University of Hyogo, Himeji, Japan.

12
13 Corresponding author: Hiroki Iwata (hiwata@shinshu-u.ac.jp)

14
15 **Key Points:**

- 16 • Diffusive and ebullitive methane fluxes from a shallow lake were examined for their
17 environmental controls at a sub-daily time scale.
- 18 • Diffusive flux was controlled by wind speed and transfer of accumulated dissolved
19 methane from the bottom layer to the surface layer.
- 20 • In addition to triggers related to wind and pressure, the accumulation of bubbles in the
21 sediment is an important factor for ebullition.
22

23 **Abstract**

24 Environmental controls on methane (CH₄) emission from lakes are poorly understood at sub-
25 daily time scales due to a lack of continuous data, especially for ebullition. We used a novel
26 technique to partition eddy covariance CH₄ flux observed in the littoral zone of a mid-latitude
27 shallow lake in Japan and examined the environmental controls on diffusive and ebullitive CH₄
28 flux separately at a sub-daily time scale during different seasons. Both diffusive and ebullitive
29 flux were significantly higher in summer than winter. The contribution of ebullitive flux to total
30 flux was 56% on average. Diffusive flux increased with increasing wind speed due to increased
31 subsurface turbulence. For a given wind speed, diffusive flux was higher in summer than in
32 winter due to the higher concentration of dissolved CH₄ in the surface water during summer. The
33 transfer of accumulated dissolved CH₄ from the bottom layer to the surface in summer and the
34 accumulation of dissolved CH₄ under surface ice in winter were important for explaining the
35 variability of diffusive flux. In summer, ebullition tended to occur following triggers such as a
36 decrease in hydrostatic pressure or an increase in wind speed. In winter, on the other hand, the
37 impact of triggers was not obvious, and ebullition tended to occur in the morning when the wind
38 speed began to increase. The low CH₄ production rate in winter slowed the replenishment of
39 bubbles in the sediment, negating the effect of triggers on ebullition.

40 **Plain Language Summary**

41 Lakes are one of the main natural sources of methane (CH₄). Methane is emitted from lake
42 sediments to the atmosphere via diffusion through the water column and episodic emission of
43 bubbles (ebullition). To improve prediction of CH₄ emission from lakes, it is necessary to clarify
44 the environmental controls on CH₄ emission processes. However, environmental controls at sub-
45 daily time scales are poorly understood due to a lack of continuous data, especially for ebullition.
46 We applied a novel technique to partition continuous CH₄ flux data obtained with the eddy
47 covariance technique in a mid-latitude shallow lake into diffusive and ebullitive fluxes, and
48 examined their environmental controls separately. The diffusive flux increased with increasing
49 wind speed and increasing dissolved CH₄ concentrations in the surface water. For this shallow
50 lake, the transfer of accumulated dissolved CH₄ from the bottom layer to the surface under
51 thermally stratified conditions was important for explaining the variability of diffusive flux. In
52 summer, ebullition tended to occur following triggers such as a decrease in hydrostatic pressure
53 or an increase in wind speed. In winter, on the other hand, the low CH₄ production rate slowed
54 the replenishment of bubbles in the sediment, negating the effect of triggers on ebullition.

55

56 **1 Introduction**

57 Lakes are one of the main natural sources of methane (CH₄), which is an important
58 greenhouse gas (e.g., Forster et al., 2007). Using bottom-up approaches, a recent global synthesis
59 estimated CH₄ emissions from fresh waters as 60-180 Tg CH₄ year⁻¹ (Saunio et al., 2016).
60 However, considerable uncertainty remains, partly stemming from the large spatiotemporal
61 variability of CH₄ emissions from lakes. Therefore, elucidating the variation and underlying
62 mechanisms of emissions is necessary to address this uncertainty.

63 CH₄ is mainly produced in anoxic lake sediments by methanogenic bacteria and is
64 emitted to the atmosphere via three emission pathways: diffusion within the water column,

65 diffusion within plant aerenchyma, and ebullition (bubble emission). These emissions are
66 controlled by different physical and biological constraints (e.g., Bastviken et al., 2004).

67 Diffusive emission at the air–water interface is strongly affected by wind speed because
68 increased wind speed results in enhanced subsurface turbulence through formation of velocity
69 shear in surface waters and waves (Cole and Caraco, 1998; Bock et al., 1999), which increases
70 the emission efficiency. In addition to wind speed, thermal instability within the water column
71 due to surface cooling increases subsurface turbulence (MacIntyre et al., 2010; Tedford et al.,
72 2014; Heiskanen et al., 2014). Diffusion also depends on the concentration difference between
73 the water surface skin layer and the bulk surface water below (Wanninkhof et al., 2009). The
74 concentration of dissolved CH₄ in the surface water is controlled by seasonal variation in CH₄
75 production in the sediments (Thebrath et al., 1993; Liikanen et al., 2003) and CH₄ oxidation
76 within the water column (Utsumi et al., 1998; Schubert et al., 2012), as well as by water mixing.
77 Water mixing is affected by wind and thermal instability of the water. During stably stratified
78 periods following surface ice formation, CH₄ produced in the sediments is trapped below the
79 thermocline. Subsequently, during periods of whole-lake mixing after ice melt, the accumulated
80 dissolved CH₄ is transported to the lake surface, enhancing emission to the atmosphere (Jammet
81 et al., 2015; Podgrajsek et al., 2016; Jansen et al., 2019).

82 Ebullition is thought to occur (1) when the sediment is disturbed by physical stress,
83 assuming that bubbles have accumulated in the sediment, or (2) when bubbles reach a
84 sufficiently large size to become buoyant. Momentum transfer to the lake sediment layer, driven
85 by wind or an internal seiche introduces physical stress to the sediment, which can force bubbles
86 to be released (Joyce and Jewell, 2003). Bubbles can grow through physical expansion due to
87 hydrostatic pressure and temperature changes and addition of gases when decreasing hydrostatic
88 pressure and/or warming sediments reduced gas solubility (e.g., Fechner-Levy and Hemond,
89 1996; Tokida et al., 2007; Wik et al., 2013).

90 CH₄ emission from lakes and its environmental controls have been traditionally examined
91 using floating chambers or bubble traps. Due to the small spatial coverage and limited time
92 resolution of these methods, however, it is difficult to obtain spatiotemporally representative flux
93 data and to clarify environmental controls in details, especially for highly variable ebullition.
94 Emissions are often controlled in a nonlinear fashion, suggesting that data with high temporal
95 resolution are necessary to elucidate detailed control mechanisms. Conversely, the eddy
96 covariance technique enables us to obtain data of continuous flux originating from a larger
97 footprint, rendering it useful for quantifying temporally and spatially variable CH₄ emissions
98 from a lake, including diffusive and ebullitive emissions.

99 Sub-daily variation in CH₄ flux from lakes and reservoirs has been reported in previous
100 eddy covariance studies (Eugster et al., 2011; Podgrajsek et al., 2014; Deshmukh et al., 2014;
101 Jammet et al., 2017; Rey-Sanchez et al., 2018). Studies in boreal lakes have reported diurnal
102 variations with a peak early in the morning (Podgrajsek et al., 2014; Jammet et al., 2017),
103 whereas studies in hydropower reservoirs observed a maximum when the artificially controlled
104 water level was lowest. Deshmukh et al. (2014) reported a clear diurnal bimodal pattern, with the
105 first peak occurring around noon and the second at midnight, whereas Eugster et al. (2011)
106 reported a maximum in the evening. These authors speculated that the maximum emissions
107 reflected an increase in ebullition.

108 One limitation of the eddy covariance technique is that it cannot distinguish emission
109 pathways, which was responsible, in part, for the ambiguous interpretation of environmental
110 controls on flux in previous studies. Recently, we developed a technique to partition eddy
111 covariance CH₄ flux into diffusive and ebullitive fluxes (Iwata et al., 2018); this technique has
112 the potential to elucidate environmental controls of diffusive and ebullitive CH₄ emissions at
113 sub-daily time scales. In addition, in most lake models (Subin et al., 2012; Stepanenko et al.,
114 2016), these emission pathways are explicitly represented at sub-daily time scales; thus, the
115 partitioned flux data are useful to parameterize and validate these lake models.

116 In this study, we applied this partitioning technique to CH₄ flux measured with the eddy
117 covariance technique for a whole year in the littoral zone of a mid-latitude shallow eutrophic
118 lake in Japan. The objectives were to quantify the contributions of diffusive and ebullitive flux in
119 the littoral zone, examine the controlling mechanisms of diffusive and ebullitive fluxes
120 separately at a sub-daily time scale, and determine whether the controls vary by seasons.

122 **2 Observation and Data Analysis**

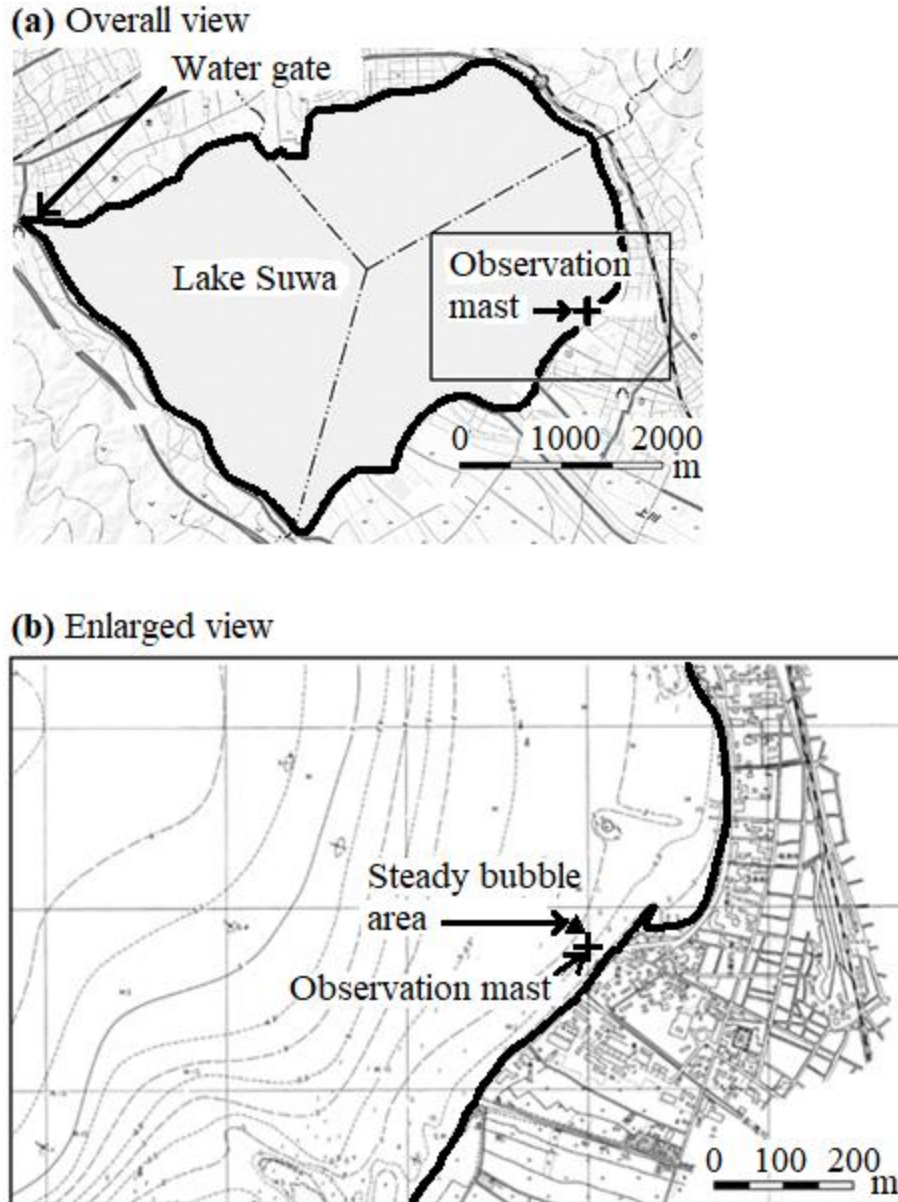
123 **2.1 Study site**

124 Measurements were conducted at the southeast shore of Lake Suwa (Fig. 1), a shallow
125 eutrophic lake located at 759 m a.s.l. in the center of Nagano Prefecture, Japan (Park et al., 1998;
126 Ikenaka et al., 2005). The total area of the lake is 13.3 km², and the mean and maximum depths
127 are approximately 4 m and 6.9 m, respectively. The water level is artificially controlled by a
128 water gate and is generally 0.2 m higher in winter than in summer. Around the observation site,
129 water caltrop (*Trapa japonica* Flerow, a floating-leaved plant) and Esthwaite waterweed
130 (*Hydrilla verticillata* [L.f.] Royle, a submerged plant) can be seen near the lake shore during
131 summer. A notable feature of this lake is that there are areas of continuous bubble emission, one
132 of which is located 55 m from the observation mast at a direction of 325° (Fig. 1b, Iwata et al.,
133 2018).

134 The lake is surrounded by cities with a combined population of more than 180,000
135 inhabitants; thus, the lake receives considerable anthropogenic inputs. Dense algal blooms are
136 regularly observed during the summer (Park et al., 1998).

137 The annual mean air temperature (1988–2017) in this area is 11.3°C; the January and
138 August monthly means are −1.0°C and 23.9°C, respectively. The mean annual precipitation is
139 1,310 mm. Figure S1 shows the distribution of wind directions during winter (from December
140 2017 to February 2018) and summer (from June to August 2018). The prevailing wind was
141 northwesterly for the lake side from the observation mast.

142



143
 144 **Figure 1.** The (a) overall and (b) enlarged view of Lake Suwa. The plus in both maps represents
 145 the location of the observation mast. The triangle in (b) represents an area with steady bubble
 146 emission (Iwata et al., 2018). The figure is produced based on a map published by the Geospatial
 147 Information Authority of Japan.
 148

149 2.2 Observations

150 Measurements were conducted from a pier (36°2'47.66"N, 138°6'30.07"E) on the
 151 southeast shore of the lake, where the water depth was approximately 2 m. The installed eddy-
 152 covariance system consisted of an ultrasonic anemo-thermometer (CSAT3; Campbell Scientific,
 153 Logan, UT, USA), open-path CH₄ analyzer (LI-7700; Li-Cor, Lincoln, NE, USA), open-path
 154 carbon dioxide (CO₂) / water vapor (H₂O) analyzer (EC-150; Campbell Scientific), and data
 155 logger (CR3000; Campbell Scientific). The observation height was about 3.2 m during summer,

156 though it changed depending on water level during the observation period. The horizontal
157 distances of the sensors from the ultrasonic anemo-thermometer were 0.25 m for the CH₄
158 analyzer and 0.05 m for the CO₂/H₂O analyzer. Footprint analysis using a model from Kormann
159 and Meixner (2001) indicated that the 90% flux footprint was typically 300–500 m from the
160 observation mast, so the observed flux represents the emission from the littoral zone of this lake.

161 Along with eddy covariance measurements, we obtained meteorological and limnological
162 data. Using the same data logger, we recorded 30-min means of wind speed (CSAT3), radiation
163 balance (CNR4; Kipp and Zonen, Delft, The Netherlands), atmospheric pressure (PTB110;
164 Vaisala, Helsinki, Finland), air temperature (HMP60; Vaisala), water and sediment temperature
165 profiles (107; Campbell Scientific), and water level (CS451; Campbell Scientific). The water
166 temperature was observed at five depths: 0.25, 0.5, 1.0, and 1.5 m below the water surface and
167 0.2 m above the local lake bottom. The top four sensors were attached to a wood pole with a
168 float so that the measurement depth was constant regardless of water-level change. The sediment
169 temperature was observed at depths of 0.05 and 0.2 m.

170 To measure dissolved CH₄ concentration, we manually sampled the water at seven depths
171 (0, 0.1, 0.5, 1.0, 1.3, and 1.5 m below the water surface and 0.2 m above the local lake bottom) at
172 approximately 1-month time intervals. Water samples at each depth were collected in three 30-
173 mL glass vials using a silicon tube and a syringe, and dissolved CH₄ concentration was measured
174 using the headspace technique (Itoh et al., 2015) with a gas chromatograph (GC-14B; Shimazu,
175 Kyoto, Japan). Finally, we calculated dissolved CH₄ concentration at each depth using the ideal
176 gas law and Bunsen solubility coefficient (Magen et al, 2014) and averaged the values from the
177 three samples. The readers are referred to Iwata et al. (submitted) for more details. In this study,
178 the surface (0 m) and bottom (0.2 m above the local lake bottom) data were used to explain the
179 seasonal variation in diffusive flux.

180

181 2.3 Flux calculation and data analysis

182 The diffusive and ebullitive CH₄ fluxes were calculated for each 30-min period using the
183 eddy covariance technique with flux partitioning (Iwata et al., 2018). Before the calculation,
184 data spikes were removed (Vickers and Mahrt, 1997). Coordinate rotation of the observed wind
185 vectors was performed so that the mean lateral and vertical wind velocities were equal to zero for
186 each 30-min period. Data from the CH₄ and CO₂/H₂O analyzer were synchronized with those
187 from sonic anemometer using cross-correlation analysis (Iwata et al., 2014). The 10 Hz data
188 were then corrected point by point (Detto and Katul, 2007, Detto et al., 2011) for the effect of
189 water vapor density on sonic virtual temperature (Schotanus et al., 1983) and for the air density
190 variation (Webb et al., 1980) and spectroscopic effects (McDermitt et al., 2011) on CH₄ density.
191 Then, a partitioning method developed in Iwata et al. (2018) was applied to calculate diffusive
192 and ebullitive CH₄ fluxes.

193 This partitioning method uses the scalar similarity concept between CH₄ molar density
194 and other reference scalars in the wavelet time-scale domain. It assumes that turbulent
195 fluctuation in CH₄ density, similar to a reference scalar with a spatially homogeneous source, is
196 due to diffusive emission, and ebullitive emission locally violates that similarity. We selected
197 H₂O density as the reference scalar, because the fluctuation of H₂O density is less affected by
198 non-local atmospheric processes, such as entrainment and advection, than that of temperature at

199 this site (Iwata et al., 2018). To separate the diffusive and ebullitive components, wavelet
200 coefficients for CH₄ density and H₂O density were compared in a scatter plot, and coefficients
201 deviating from a regression line fitted to the coefficients were considered ebullitive components.
202 For each month, we determined root mean squared deviations (RMSDs) around the regression
203 line from visually selected 30-min 10 Hz data (n = 4) in which H₂O density and CH₄ density had
204 global similarity. Assuming that the deviations from the regression line were normally
205 distributed, we defined coefficients inside and outside $\pm 3 \times \text{RMSD}$ bounds corresponding to
206 diffusive and ebullitive flux, respectively.

207 The analysis was conducted for data obtained from September 2017 to August 2018. We
208 used only flux data with wind blowing from 230–300° to eliminate data affected by the land
209 surface and steady CH₄ bubble emission. The fluxes obtained from this sector showed low
210 spatial variation with large episodic fluxes (Iwata et al. submitted), representing littoral CH₄
211 emission typical of similar lakes. General quality control (Vickers and Mahrt, 1997; Mahrt,
212 1998) was applied to assure flux data quality. Additionally, data affected by possible non-local
213 processes were removed from the analysis because non-local processes can affect the scalar
214 similarity, making the partitioning ambiguous. The effect of non-local processes was
215 investigated in the flux–variance relationship (De Bruin et al., 1993; van de Boer et al., 2014) for
216 H₂O density, where data deviating from the universal function with locally adjusted parameters
217 were removed. Data with ebullitive flux $< 0 \mu\text{mol m}^{-2} \text{s}^{-1}$ or diffusive flux $< -0.05 \mu\text{mol m}^{-2} \text{s}^{-1}$
218 (137 data points) were also eliminated. The data processing and selection criteria left 2,647
219 diffusive and ebullitive flux data points (15% of the whole) remaining for the analysis. In this
220 manuscript, data from December 2017 to February 2018 represent winter, and data from June to
221 August 2018 represent summer, unless otherwise specified.

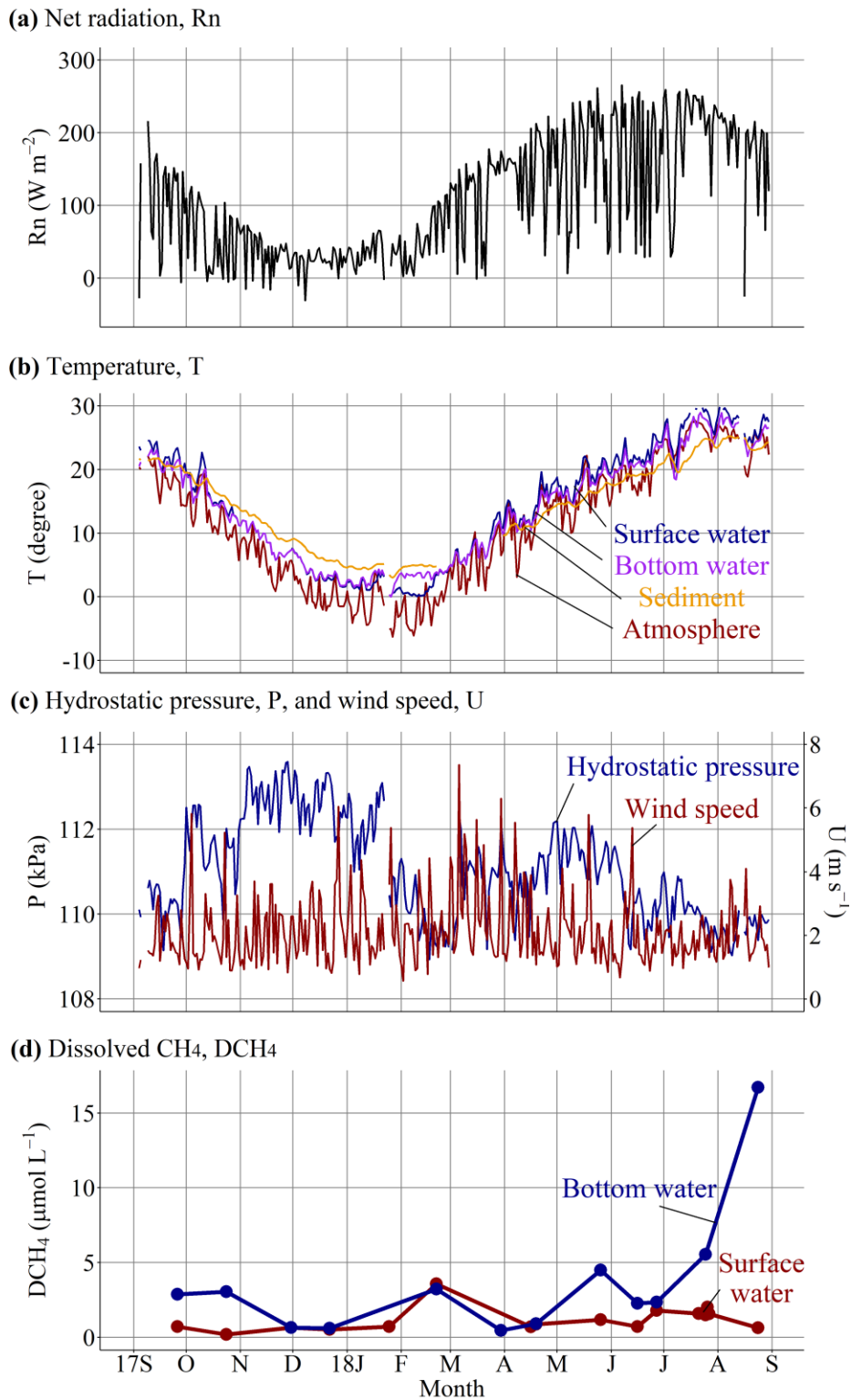
222

223 **3 Results and Discussion**

224 3.1 Meteorological and limnological conditions

225 In summer, the daily average lake surface temperature was higher than the bottom
226 temperature by 0.2–4.0°C (Fig. 2b), indicating that the lake was stably stratified when net
227 radiation was high (Fig. 2a). During winter, the lake surface and bottom temperatures were
228 nearly identical, indicating that the lake was well mixed, except from late January to the middle
229 of February. During that period, the lake surface was frozen, and the surface temperature was
230 close to zero, whereas the bottom temperature was about 4°C, resulting in stable stratification.
231 Hydrostatic pressure was, on average, higher in winter than in summer (Fig. 2c), mainly because
232 the water level was artificially maintained at a greater depth in winter than in summer by a water
233 gate. Additionally, week-scale fluctuations of hydrostatic pressure were observed, which were
234 mainly caused by passage of low- and high-atmospheric-pressure systems. The wind speed
235 tended to be higher in March–April on average, and sudden increases in daily mean wind speed
236 coincided with the passage of strong low-pressure systems. The dissolved CH₄ concentration was
237 higher in summer for both the surface and bottom layer (Fig. 2d). Dissolved CH₄ accumulated
238 during summer, especially in the bottom layer, because of stable stratification. Data obtained
239 after surface ice melt in February showed increased concentrations for both the surface and
240 bottom layer. This accumulation was caused by the physical blockage of CH₄ diffusion to the
241 atmosphere by the surface ice.

242



243

244 **Figure 2.** Seasonal variations in (a) net radiation; (b) temperatures of air (red), surface water
 245 (0.25 m depth: blue), bottom water (0.2 m above the local lake bottom: purple), and sediment
 246 (0.2 m depth: orange); (c) hydrostatic pressure (blue) and wind speed (red); and (d) dissolved

247 CH₄ concentration in the surface (0 m depth: red) and bottom (0.2 m above the local lake bottom:
248 blue) layer.

249

250 3.2 Seasonal variations in diffusive and ebullitive methane flux

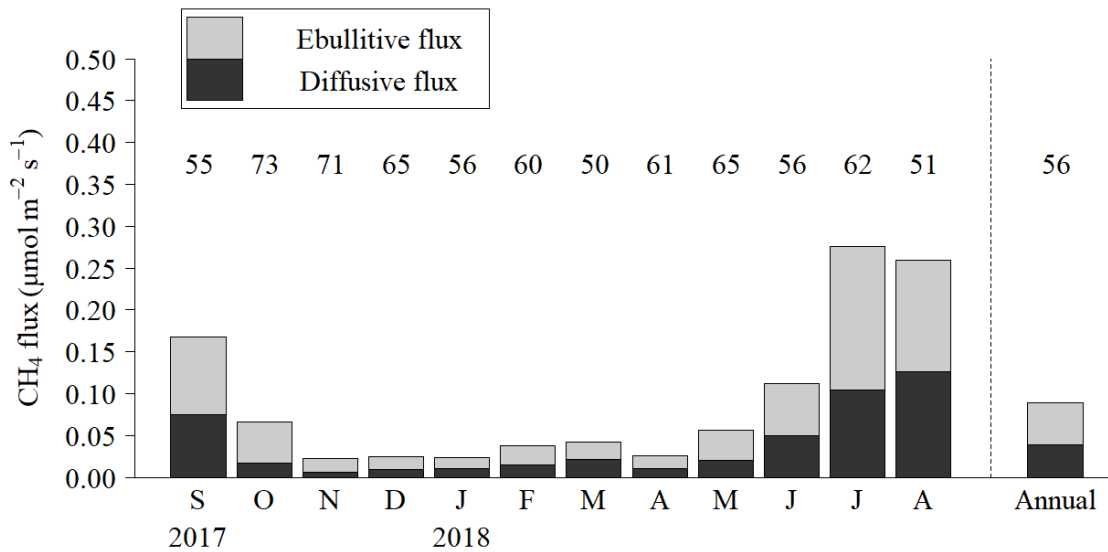
251 Both diffusive and ebullitive CH₄ flux were significantly higher in summer than in winter
252 (Fig. 3). Mean diffusive CH₄ fluxes in winter and summer were 0.01 and 0.09 $\mu\text{mol m}^{-2} \text{s}^{-1}$,
253 respectively, and mean ebullitive CH₄ fluxes in winter and summer were 0.02 and 0.12 $\mu\text{mol m}^{-2}$
254 s^{-1} , respectively. Incubation experiments using sediments from the same lake (Iwata et al.,
255 submitted) and other lakes (Duc et al., 2010) have shown that higher sediment temperatures in
256 summer can enhance CH₄ production in the sediment, thereby increasing diffusive and ebullitive
257 fluxes in summer.

258 Diffusive CH₄ flux had a relatively normal distribution: the skewness was -0.19 and 1.31
259 for winter (January 2018) and summer (July 2018), respectively (Fig. S2). The ebullitive CH₄
260 flux in winter had a positively skewed distribution (skewness, 7.14), whereas the distribution in
261 summer was relatively normal (1.21). The high positive skewness in winter indicates that the
262 larger ebullitive flux in winter occurred more episodically than that in summer.

263 Ebullitive CH₄ flux contributed 60% of the total flux in winter, 57% in summer, and 56%
264 annually, showing that both diffusion and ebullition are dominant pathways of CH₄ emission in
265 this shallow lake. Generally, ebullitive flux is thought to contribute 40–60% of total fluxes from
266 open water, and its contribution to total flux decreases with increasing lake size (Bastviken et al.,
267 2004). In a study conducted in three lakes and ten ponds in northern North America, ebullitive
268 CH₄ flux accounted for 18–23% of the total CH₄ fluxes for lakes, and ~56 % of total flux for
269 ponds (DelSontro et al., 2016). Conversely, in a meta-analysis (Bastviken et al., 2011), the
270 relative contributions of ebullition were much higher on average (70–90%) for lakes across all
271 latitude bands. The episodic nature of ebullition is probably responsible for the considerable
272 uncertainty in estimations of its relative contributions. It should be noted that the CH₄ flux
273 observed in our lake represents emission from the littoral zone, where ebullition is known to
274 occur more frequently than in the pelagic deep zone due to higher CH₄ production and lower
275 hydrostatic pressure (DelSontro et al., 2016; Itoh et al., 2017). Thus, the contribution of
276 ebullition may be lower when also accounting for CH₄ flux in the pelagic zone of this lake.

277 To roughly estimate the annual total emission from Lake Suwa, we assumed that the
278 mean diurnal variations in diffusive and ebullitive fluxes for each month obtained from the
279 selected data were representative of the flux for the whole month. Based on the mean diurnal
280 variations, mean daily fluxes for each month were calculated and multiplied by the amount of
281 time in the month to deduce the monthly total flux. Thus, by then summing over 12 months, we
282 obtained annual CH₄ fluxes of 17.6 and 19.3 $\text{g CH}_4 \text{m}^{-2} \text{year}^{-1}$ for diffusion and ebullition,
283 respectively, and a total flux of 36.9 $\text{g CH}_4 \text{m}^{-2} \text{year}^{-1}$.

284



285
 286 **Figure 3.** Seasonal variations in diffusive (black bar) and ebullitive (grey bar) CH₄ fluxes. The
 287 numbers above the bar indicate the contribution (%) of ebullitive flux to the total CH₄ flux (i.e.,
 288 diffusive plus ebullitive flux). The rightmost bar shows the annual average calculated as the
 289 average of monthly averages.

290

291 3.3 Sub-daily variation in diffusive flux

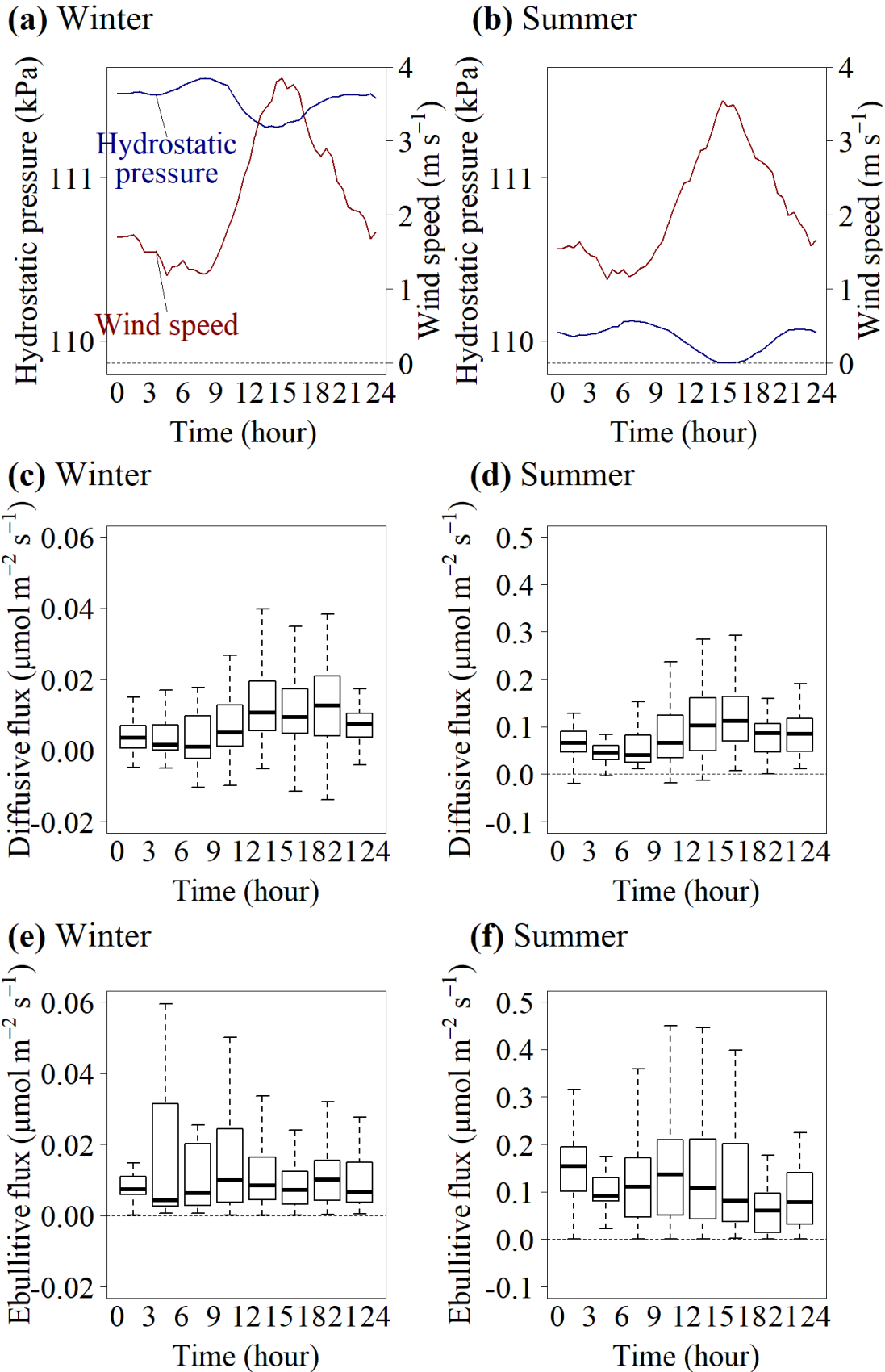
292 At a sub-daily time scale, diffusive flux was high in the afternoon (Fig. 4c, d) in both
 293 summer and winter when wind speed increased (Fig. 4a, b). Sediment temperature was not a
 294 significant controlling factor of CH₄ flux at a sub-daily time scale, because its diurnal variation
 295 was <1.0°C throughout the observation period (Fig. S3). Diffusive flux in other seasons also
 296 showed a similar tendency. The relationship between diffusive flux and wind speed (Fig. 5)
 297 confirmed the wind speed dependency. This wind speed dependence was consistent with
 298 previous studies, including a floating chamber observations in Liu et al. (2017) and gas-transfer
 299 velocity studies (Guérin et al., 2007; Heiskanen et al., 2014). Subsurface turbulence is enhanced
 300 by increasing wind speed (e.g., Wanninkhof et al., 2009), which explains the dependence of
 301 diffusive flux on wind speed.

302 For a given wind speed, the diffusive flux was higher in summer (Fig. 5). This is due to
 303 the difference in mean dissolved CH₄ concentration in the surface water caused by the seasonal
 304 variation of CH₄ production; the dissolved CH₄ concentration in the surface water derived from
 305 observations at one-month intervals (Fig. 3d) was 0.72 μmol L⁻¹ in winter (January 25, 2018)
 306 and 1.49 μmol L⁻¹ in summer (July 25, 2018). It should be noted that these data are not
 307 necessarily typical for the month because the mixing caused by strong wind can lead to a high
 308 variation of dissolved CH₄ concentration, even during stable stratification in summer due to the
 309 transfer of dissolved CH₄ from the bottom layer in this shallow lake. Formation of surface ice
 310 also led to the accumulation of dissolved CH₄ during winter (Fig. 3d). These unobserved
 311 variations in surface dissolved CH₄ concentration may partly explain the variability shown in
 312 Fig. 5.

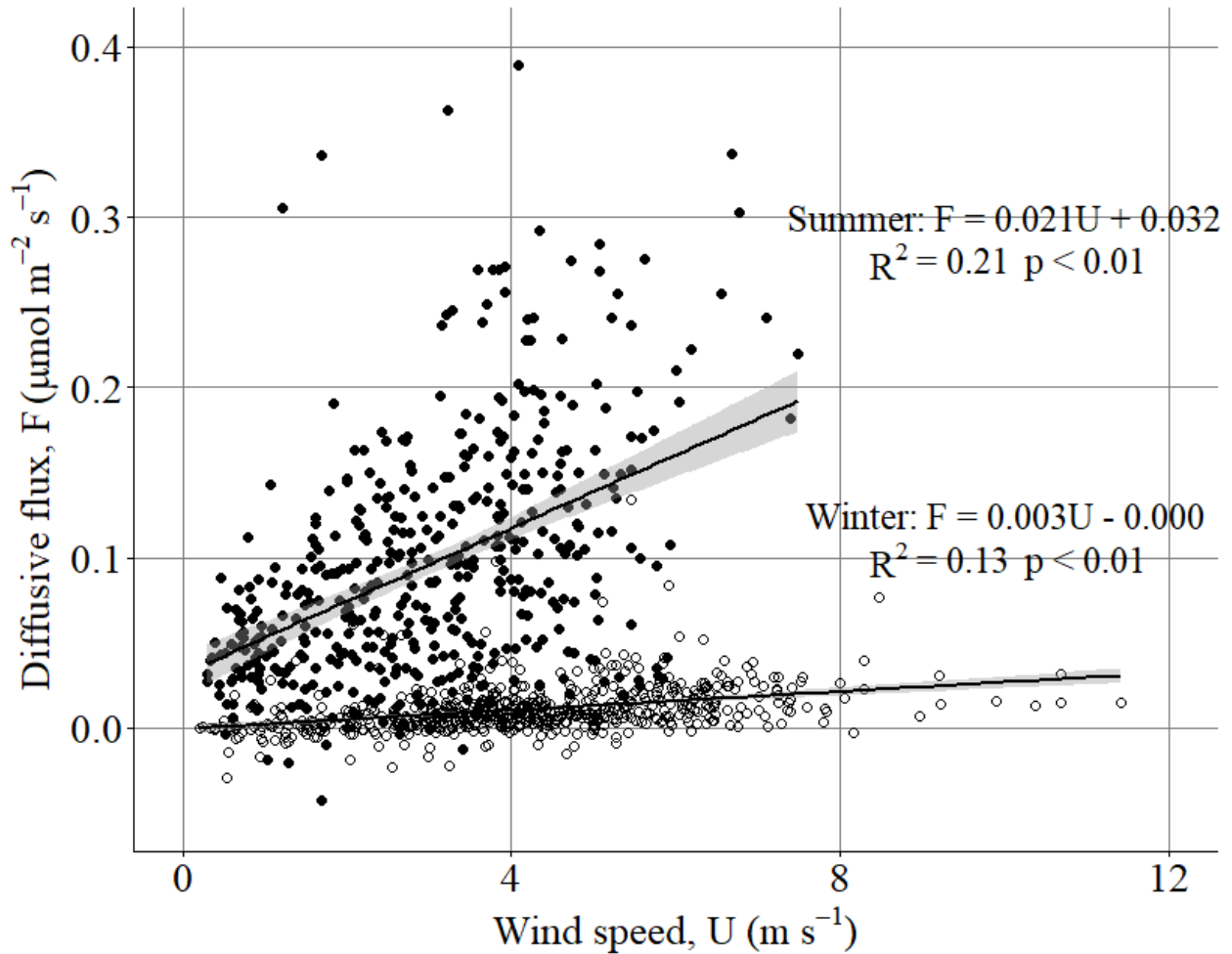
313 To examine the effect of variation in surface dissolved CH₄ concentration on diffusive
314 flux, we separated the winter data into periods before surface ice formation and after ice melt
315 (Fig. 6a). After ice melt on February 22, the increase in diffusive flux with increasing wind speed
316 was higher than before ice formation. This was probably due to the high concentration of
317 dissolved CH₄ in the surface water after ice melt. The concentration of dissolved CH₄ in the
318 surface water on February 21 (i.e., immediately before the ice melt was complete) was $3.58 \pm$
319 $0.15 \mu\text{mol L}^{-1}$ (Fig. 3d), which was the highest value observed in the surface water during the
320 study period. When the lake was covered with surface ice (January 27–February 21, 2018),
321 diffusive flux was poorly explained by wind speed ($R^2 = 0.03$, Fig. S4). Higher flux was also
322 observed during this period, likely caused by emissions through melted areas of the surface ice.

323 To examine the relationship of diffusive flux with wind speed during summer, the data
324 were separated based on the mean wind speed of the preceding 24 hours (Fig. 6b). When the
325 mean wind speed was low during the preceding 24 hours, it was assumed that dissolved CH₄
326 accumulated in the bottom layer, a condition under which the potential for diffusion increases.
327 We found that diffusive flux was higher for a given current wind speed when wind was calmer
328 during the preceding 24 hours. This suggests that the transfer of accumulated dissolved CH₄
329 from the bottom layer is an important factor influencing diffusive flux.

330 In the transfer velocity model, diffusive flux is estimated from the difference in
331 concentration between the thin surface water layer and the bulk surface water below. CH₄
332 concentration in surface water generally changes at sub-daily time scales in shallow lakes;
333 however, data on continuously measured dissolved CH₄ concentrations are scarce due to
334 technical constraints (e.g., Erkkilä et al., 2018). Therefore, continuous measurement of dissolved
335 CH₄ concentration is needed to evaluate the impacts of ice sheets during winter and transport of
336 CH₄-enriched bottom-layer water during summer on diffusive CH₄ emission from shallow lakes.
337

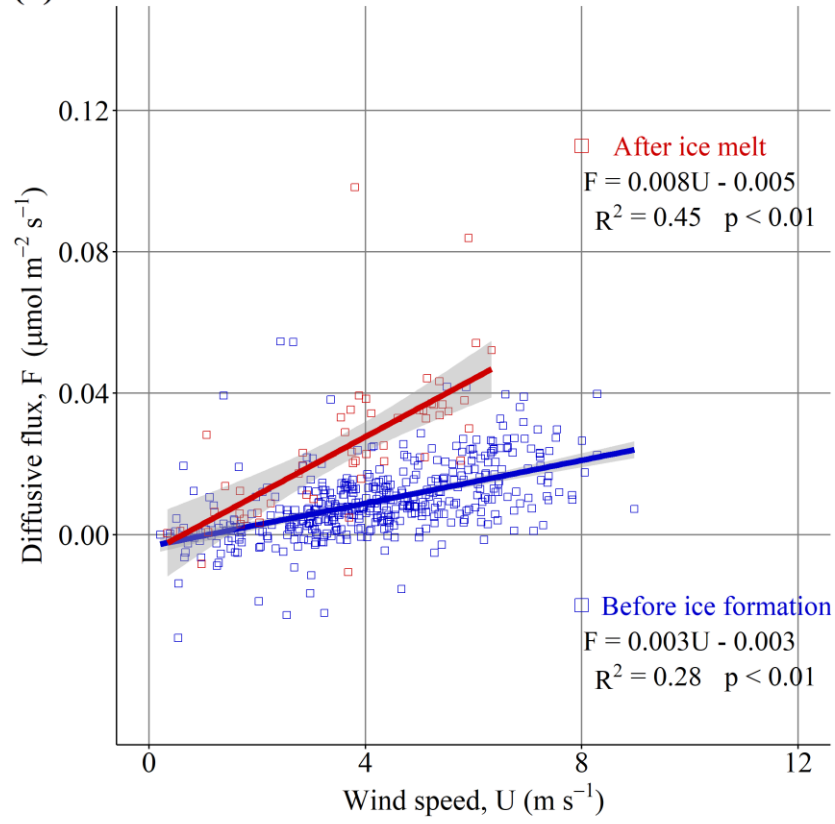


339 **Figure 4.** Mean diurnal variation in (a, b) hydrostatic pressure (blue) and wind speed (red), (c, d)
 340 diffusive flux, and (e, f) ebullitive flux for winter (left panels) and summer (right panels). In the
 341 boxplots of (c–f), the center lines represent median values, and the widths of the boxes show the
 342 interquartile ranges (IQR), and the whiskers represent maximum and minimum values within a
 343 range of median $\pm 1.5 \times$ IQR. Data outside the range of the whiskers were not shown in these
 344 plots.
 345

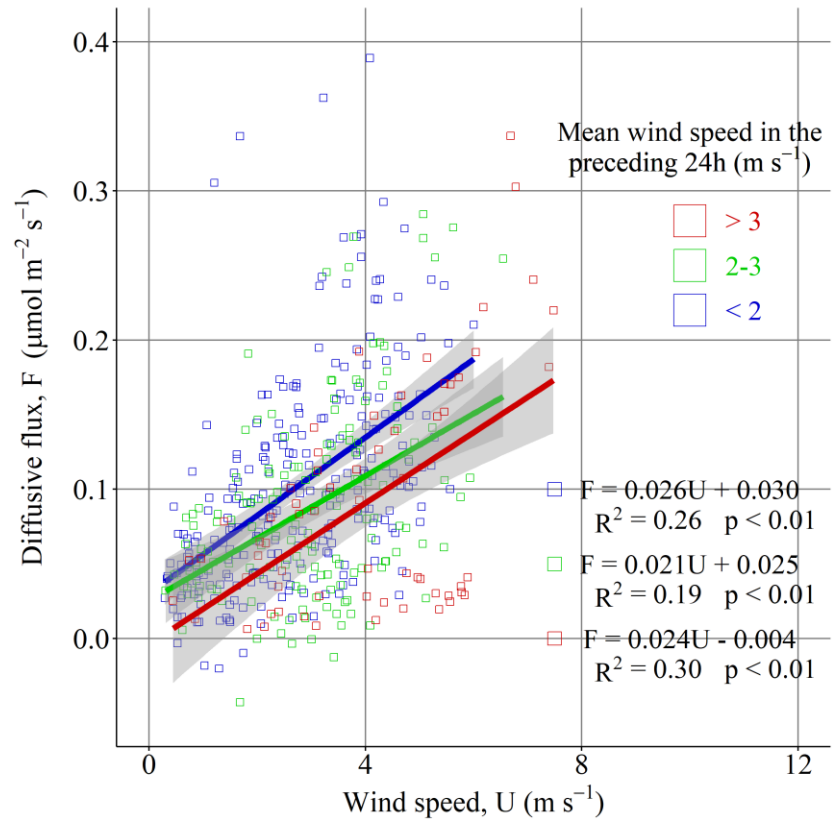


346 **Figure 5.** The relationship between wind speed and diffusive flux in winter (open circle) and
 347 summer (solid circle). Gray zones indicate 95% confidence intervals.
 348
 349

(a) Winter



(b) Summer



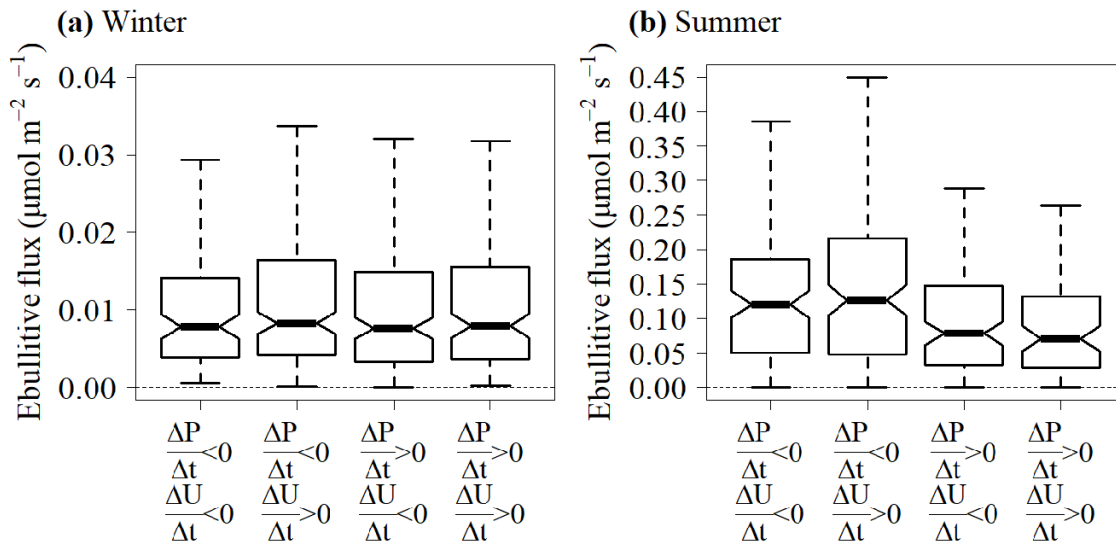
351 **Figure 6.** The relationship between wind speed and diffusive flux in (a) winter and (b) summer.
 352 (a) In winter, the data were separated into periods before surface ice formation (December 1 to
 353 January 26, blue points) and after ice melt (February 22 to 28, red points). (b) In summer, data
 354 were separated according to mean wind speed in the preceding 24 hours: blue points for $<2 \text{ m}$
 355 s^{-1} , green points for $2\text{--}3 \text{ m s}^{-1}$, and red points for $>3 \text{ m s}^{-1}$. Gray zones indicate 95% confidence
 356 intervals.
 357

358 3.4 Short-term variation in ebullitive flux

359 In winter, higher ebullition was more frequently observed in the morning (3:00–12:00)
 360 (the upper quartile and whisker in Fig. 4e), with few high-flux observations in the afternoon
 361 (12:00–18:00). Ebullitive flux increased when wind speed began to increase (Fig. 4a), implying
 362 that wind was as a trigger for ebullition. However, ebullitive flux was not always high in the
 363 morning, as the median value was comparable to those for other time periods. In summer, no
 364 clear diurnal variation was observed for peak ebullitive flux (Fig. 4f), although the median values
 365 during 0:00–3:00 and 9:00–12:00 were slightly higher, and those during 3:00–6:00 and 18:00–
 366 21:00 slightly lower, than in other time periods. These slightly higher and lower ebullitive fluxes
 367 occurred during times of decreasing and increasing hydrostatic pressure, respectively, caused by
 368 atmospheric tides (Fig. 4b).

369 The responses of ebullitive flux to 30-min changes in wind speed and hydrostatic
 370 pressure were examined to elucidate environmental controls on ebullitive flux in detail (Fig. 7).
 371 When calculating the change in wind speed, wind speed data were smoothed using 5.5-h moving
 372 average before subtraction. In summer, the median and upper quartile of ebullitive flux were
 373 higher when hydrostatic pressure decreased ($\Delta P/\Delta t < 0$ in Fig. 7b). Increases in wind speed
 374 ($\Delta U/\Delta t > 0$) in combination with the decrease in pressure ($\Delta P/\Delta t < 0$) further enhanced ebullitive
 375 flux. These results are consistent with previous studies in which decreasing hydrostatic pressure
 376 (e.g., Tokida et al., 2007; Wik et al., 2013) and bottom shear stress caused by wind (e.g., Joyce
 377 and Jewell, 2003) were reported as triggers for ebullition. However, this pattern was not clear in
 378 winter (Fig. 7a).

379



380

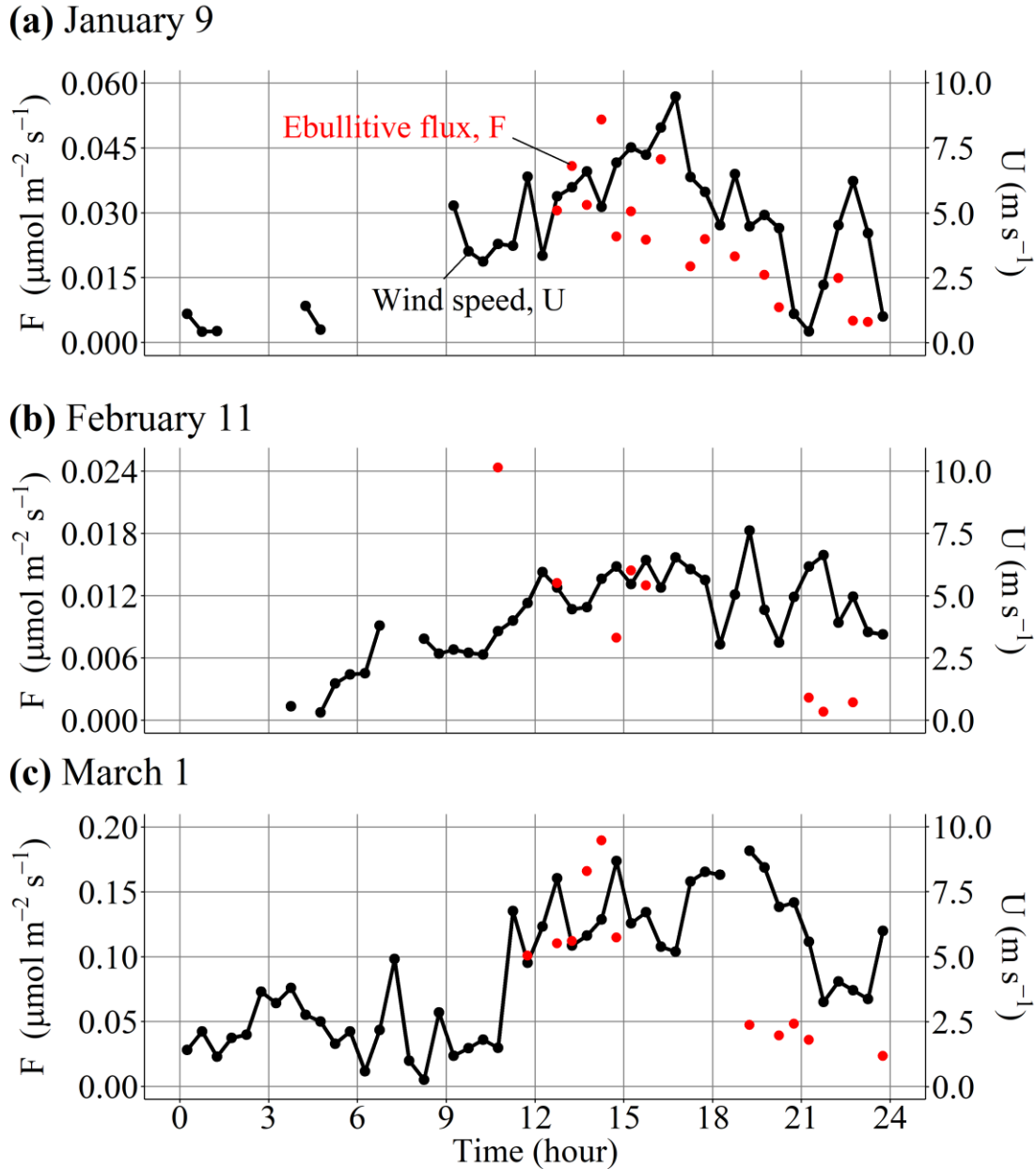
381 **Figure 7.** The effect of triggers (changes in hydrostatic pressure and wind speed) on ebullitive
382 CH₄ flux in (a) winter and (b) summer. The data were divided into groups with different
383 conditions: (1) decreasing pressure and wind speed; (2) decreasing pressure and increasing wind
384 speed; (3) increasing pressure and decreasing wind speed; and (4) increasing pressure and wind
385 speed. The boxplots are explained in the caption of **Fig. 4.** The notches represent 95%
386 confidence intervals of medians.

387

388 The dependence of ebullitive flux on the magnitude of wind speed, rather than the
389 change, was also investigated (Fig. S5). Ebullitive flux decreased with increasing wind speed in
390 winter, although such a trend was not clear in summer.

391 In addition to the direct effect of triggers on ebullitive flux, the accumulation of bubbles
392 in the sediment may be an important factor regulating the response of ebullitive flux to triggers.
393 Under strong winds during winter, a decline in ebullitive flux was observed in the afternoon
394 despite a continuous high wind speed (Fig. 8). Bubbles remaining in the sediment decrease as
395 ebullition proceeds, and low temperatures slow the replenishment of bubbles, thus limiting
396 ebullition. In summer, such a continuous decline in ebullitive flux was not observed.

397

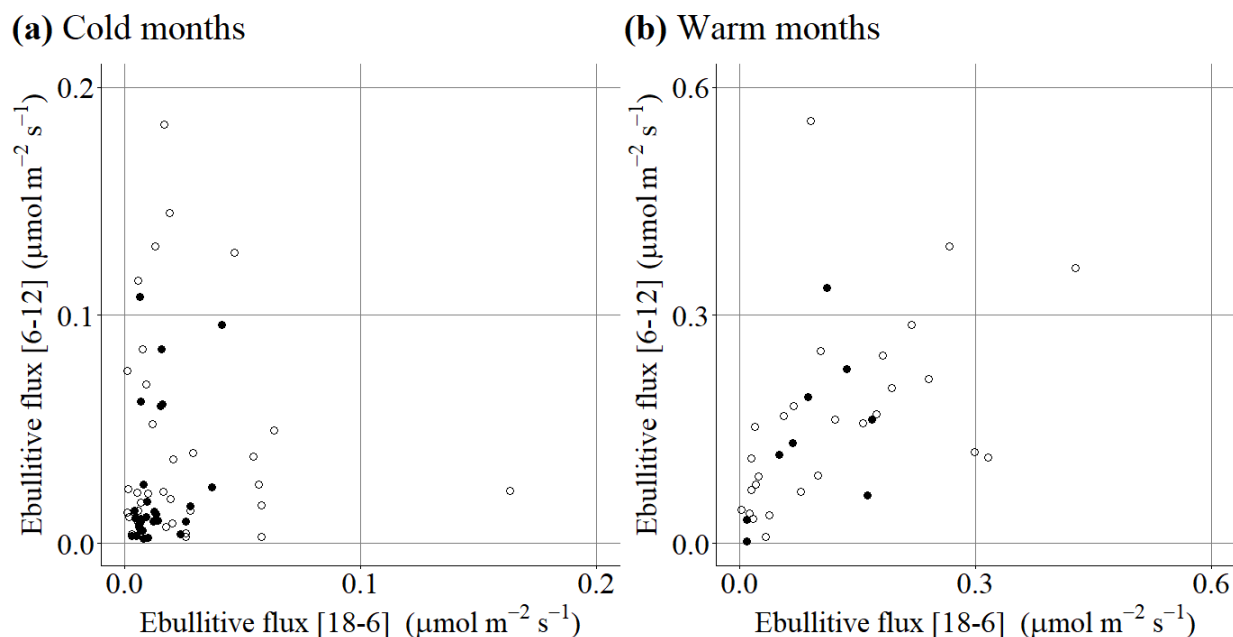


398
 399 **Figure 8.** Case studies showing the variation in ebullitive CH₄ flux (red points) with wind speed
 400 (black line) in winter. The data are for (a) January 9, (b) February 11, and (c) March 1.

401
 402 To further investigate how limited accumulation of sediment bubbles can affect
 403 ebullition, the relationships between median ebullitive flux at night (18:00–6:00) and the
 404 following morning (6:00–12:00) during cold (November–April, Fig. 9a) and warm months
 405 (May–October, Fig. 9b) were examined. In cold months, when high ebullitive flux (>0.05 μmol
 406 m⁻² s⁻¹) was observed at night, the median ebullitive flux the following morning was generally
 407 lower. By contrast, when high ebullitive flux was not observed at night, high ebullitive flux
 408 tended to be observed the following morning. These relationships confirmed that winter

409 ebullitive flux is limited by the amount of bubble accumulation in the sediment, in addition to
 410 triggers such as changes in hydrostatic pressure and wind speed. Conversely, such relationships
 411 were not observed in summer, indicating that summer ebullitive flux is less limited by the
 412 amount of bubbles in the sediment because high rates of CH₄ production driven by high
 413 temperatures continuously replenish bubbles in the sediment. We also examined the relationship
 414 between ebullition in the morning and ebullition the following afternoon and found similar
 415 results (Fig. S6), indicating limited bubble accumulation in winter.

416



417 **Figure 9.** Scatter plots of the daily median ebullitive CH₄ flux at night (18:00–6:00) and the
 418 following morning (6:00–12:00) during (a) cold months (November–December in 2017 and
 419 January–April in 2018) and (b) warm months (September–October in 2017 and May–August in
 420 2018). Black solid circles represent the median ebullitive flux with $n \geq 3$ for both the horizontal
 421 and vertical axes, while open circles represent those with $n < 3$.
 422

423

424 The limited bubble accumulation in the sediments during winter provides insights into the
 425 different observed behaviors of ebullitive flux in winter and summer (Figs. 4 and 7). In winter,
 426 bubbles can accumulate in the sediment overnight when the wind speed is generally low (Fig. 4a)
 427 and are emitted to the atmosphere when wind speed begins to increase in the morning. In the
 428 afternoon, most of the accumulated bubbles have already been emitted to the atmosphere, so
 429 fewer remain in the sediment due to the lower CH₄ production rate in winter. This can lead to
 430 relatively clear diurnal patterns in ebullitive flux in winter (Fig. 4e). In winter, the amount of
 431 bubbles in the sediment is limited due to the low CH₄ production rate, and ebullition does not
 432 always occur even with triggers such as a decrease in hydrostatic pressure or increase in wind
 433 speed (Fig. 7a). In summer, the amount of accumulated bubbles was high enough due to the high
 434 CH₄ production rate that ebullition could occur any time there was a trigger (Fig. 7b). This led to
 435 relatively obscure diurnal patterns of ebullitive flux in summer (Fig. 4f). These results suggest

436 the importance of considering bubble accumulation in the sediments to explain variation in
437 ebullitive flux at sub-daily time scales.

438 Podgrajsek et al. (2014) measured CH₄ flux using the eddy covariance technique in a
439 boreal lake and showed that CH₄ flux tended to be high in the morning during spring and fall.
440 The mean diurnal variation was similar to the variation in ebullitive flux observed at our site in
441 winter. Although the authors suggested that disturbance of the water–sediment interface through
442 convective turbulence could explain the high flux at night and early morning (Podgrajsek et al.,
443 2014), our study also highlights the necessity of considering bubbles accumulated in the
444 sediments. The similarity in diurnal variation of CH₄ flux suggests that ebullition in mid-latitude
445 lakes may be limited by a lack of bubble accumulation in the sediment during cold months.

446

447 **4 Conclusions**

448 We measured CH₄ flux with the eddy covariance technique in a shallow eutrophic lake
449 located in central Japan. We partitioned the total flux into diffusive and ebullitive fluxes, which
450 enabled us to examine their environmental controls separately and in detail.

451 Mean total CH₄ flux was 0.03 μmol m⁻² s⁻¹ in winter and 0.21 μmol m⁻² s⁻¹ in summer.
452 CH₄ flux was clearly higher in summer than winter; however, winter flux should not be ignored
453 for accurate estimation of annual CH₄ flux. Diffusive and ebullitive flux contributed 44% and
454 56%, respectively, of total CH₄ flux, on average. Thus, both diffusion and ebullition are
455 dominant pathways of CH₄ emitted to the atmosphere in this lake. Rough estimates of the annual
456 mean diffusive and ebullitive fluxes were 17.6 and 19.3 g CH₄ m⁻² year⁻¹, respectively, and total
457 flux was 36.9 g CH₄ m⁻² year⁻¹.

458 Diffusive flux increased as wind speed increased due to enhanced subsurface turbulence.
459 Diffusive flux was higher in summer than in winter due to higher dissolved CH₄ concentration in
460 the surface water. These results are consistent with those obtained using other methods such as
461 floating chambers. Additionally, the transfer of accumulated dissolved CH₄ from the bottom
462 layer to the surface in summer and accumulation of dissolved CH₄ under surface ice are
463 important processes that explain the variability of diffusive flux.

464 Ebullition occurred following triggers such as a decrease in hydrostatic pressure or an
465 increase in wind speed, consistent with previous studies. Using high time-resolution flux data,
466 we further clarified the importance of considering bubbles accumulated in the sediments to
467 explain the variation in ebullitive flux at sub-daily time scales. In winter, low CH₄ production
468 slowed the replenishment of bubbles in the sediment, limiting ebullitive flux even when triggers
469 occurred.

470 This study highlighted the power of the eddy covariance technique combined with flux
471 partitioning as a general tool for elucidating the environmental controls underlying CH₄ flux in
472 lakes, which are expected to depend on the lake properties. This will further improve our ability
473 to predict CH₄ emission from lakes under climate change.

474

475 **Acknowledgments**

476 We would like to thank Mr. Hiroshi Moriyama for allowing us to use the pier for observations.
477 This study was funded by a grant from the Japan Society for the Promotion of Science (JSPS)
478 KAKENHI (no. 17H05039). Data sets used in this research are available online
479 (<http://science.shinshu-u.ac.jp/~hiwata/program.html>).
480

481 **References**

- 482
483 Bastviken, D., Cole, J., Pace, M., and Tranvik, L. (2004), Methane emissions from lakes:
484 dependence of lake characteristics, two regional assessments, and a global estimate. *Global*
485 *Biogeochemical Cycle*, 18(4), GB4009. doi:10.1029/2004GB002238
486
487 Bastviken, D., Tranvik, L. J., Downing, J. A., Crill, P. M., Enrich-Prast A. (2011), Freshwater
488 methane emissions offset the continental carbon sink. *Science*, 331, 50.
489 doi:10.1126/science.1196808
490
491 Bock E. J., Hara, T., Frew, N. M., McGillis, W. R. (1999), Relationship between air-sea gas
492 transfer and short wind waves. *Journal of Geophysical Research*, 104(C11), 821-831.
493 doi:10.1029/1999JC900200
494
495 Cole, J. J. and Caraco, N. F. (1998), Atmospheric exchange of carbon dioxide in a low-wind
496 oligotrophic lake measured by the addition of SF₆. *Limnology and Oceanography*, 43(4), 647-
497 656. doi:10.4319/lo.1998.43.4.0647
498
499 De Bruin H. A. R., Kohsiek, W., and Van den Hurk B. J. J. M. (1993), A verification of some
500 methods to determine the fluxes of momentum, sensible heat, and water vapor using standard
501 deviation and structure parameter of scalar meteorological quantities. *Boundary-Layer*
502 *Meteorology*, 63(3), 231-257. doi:10.1007/BF00710461
503
504 DelSontro, T., Boutet, L., St-Pierre, A., Giorgio, P. A., Prairie, Y. T. (2016), Methane ebullition
505 and diffusion from northern ponds and lakes regulated by the interaction between temperature
506 and system productivity. *Limnology and Oceanography*, 61(S1), S62-S77.
507 doi:10.1002/lno.10335
508
509 Deshmukh, C., Serca, D., Delon, C., Tardif, R., Demarty, M., Jarnot, C., Meyerfeld, Y.,
510 Chanudet, V., Guédant, P., Rode, W., Descloux, S., and Guérin, F. (2014), Physical controls on
511 CH₄ emissions from a newly flooded subtropical freshwater hydroelectric reservoir: Nam
512 Theun 2. *Biogeosciences*, 11(15), 4251-4269. doi:10.5194/bg-11-4251-2014
513
514 Detto, M. and Katul, G. C. (2007), Simplified expressions for adjusting higher-order turbulent
515 statistics obtained from open path gas analyzers. *Boundary-Layer Meteorology*, 122(1), 205-216.
516 doi:10.1007/s10546-006-9105-1
517
518 Detto M., Verfaillie, J., Anderson, F., Xu, L., Baldocchi, D. (2011), Comparing laser-based
519 open- and closed-path gas analyzers to measure methane fluxes using the eddy covariance

520 method. *Agricultural and Forest Meteorology*, 151(10), 1312-1324.
521 doi:10.1016/j.agrformet.2011.05.014

522
523 Duc, N. T., Crill, P., and Bastviken, D. (2010), Implications of temperature and sediment
524 characteristics on methane formation and oxidation in lake sediments. *Biogeochemistry*, 100(1-
525 3), 185-196. doi:10.1007/s10533-010-9415-8

526
527 Erkkilä, K. M., Ojala, A., Bastviken, D., Biermann, T., Heiskanen, J. J., Lindroth, A., Peltola, O.,
528 Rantakari, M., Vesala, T., and Mammarella, I. (2018), Methane and carbon dioxide fluxes over a
529 lake: comparison between eddy covariance, floating chambers, and boundary layer method.
530 *Biogeosciences*, 15(2), 429-445. doi:10.5194/bg-15-429-2018

531
532 Eugster, W., DelSontro, T., and Sobek, S. (2011), Eddy covariance flux measurements confirm
533 extreme CH₄ emissions from a Swiss hydropower reservoir and resolve their short-term
534 variability. *Biogeosciences*, 8(9), 2815-1831. doi:10.5194/bg-8-2815-2011

535
536 Fechner-Levy, E. J. and Hemond, H. F. (1996), Trapped methane volume and potential effects
537 on methane ebullition in a northern peatland. *Limnology and Oceanography*, 41(7), 1375-1383.
538 doi:10.4319/lo.1996.41.7.1375

539
540 Forster, P., Ramaswamy, V., Artaxo, P., Berntsen, T., Betts, R., Fahey, D. W., Haywood, J.,
541 Lean, J., Lowe, D. C., Myhre, G., Nganga, J., Prinn, R., Raga, G., Schulz, M., and Van Dorland,
542 R. (2007), Changes in Atmospheric Constituents and in Radiative Forcing. In: *Climate Change*
543 *2007: The Physical Science Basis. Contribution of Working Group I to the Fourth Assessment*
544 *Report of the Intergovernmental Panel on Climate Change.* Cambridge University Press,
545 Cambridge, United Kingdom and New York, NY, USA, 129-234.

546
547 Guérin, F., Abril, G., Serça, D., Delon, C., Richard, S., Delmas, R., Tremblay, A., and Varfalvy,
548 L. (2007), Gas transfer velocities of CO₂ and CH₄ in a tropical reservoir and its river
549 downstream. *Journal of Marine Systems*, 66(1-4), 161-172. doi:10.1016/j.jmarsys.2006.03.019

550
551 Heiskanen, J. J., Mammarella, I., Haapanala, S., Pumpanen, J., Vesala, T., Macintyre, S., and
552 Ojala, A. (2014), Effects of cooling and internal wave motions on gas transfer coefficients in a
553 boreal lake. *Tellus B*, 66(1), 22827. doi:10.3402/tellusb.v66.22827

554
555 Ikenaka, Y., Eun, H., Watanabe, E., Miyabara, Y. (2005), Sources, distribution, and inflow
556 pattern of dioxins in the bottom sediment of Lake Suwa, Japan. *Bulletin of Environmental*
557 *Contamination and Toxicology*, 75(5), 915-921. doi:10.1007/s00128-005-0837-2

558
559 Itoh, M., Kobayashi, Y., Chen, T. Y., Tokida, T., Fukui, M., Kojima, H., Miki, T., Tayasu, I.,
560 Shiah, F. K., and Okuda, N. (2015), Effect of interannual variation in winter vertical mixing on
561 CH₄ dynamics in a subtropical reservoir. *Journal of Geophysical Research: Biogeosciences*,
562 120(7), 1246-1261. doi:10.1002/2015JG002972

563
564 Itoh, M., Kojima, H., Ho, P.-C., Chang, C.-W., Chen, T.-Y., Hsiao, S. S.-Y., Kobayashi, Y.,
565 Fujibayashi, M., Kao, S.-J., Hsieh, C., Fukui, M., Okuda, N., Miki, T., and Shiah, F.-K. (2017),

- 566 Integrating isotopic, microbial, and modeling approaches to understand methane dynamics in a
567 frequently disturbed deep reservoir in Taiwan. *Ecological Research*, 32(6), 861-871,
568 doi:10.1007/s11284-017-1502-z
- 569
- 570 Iwata, H., Kosugi, Y., Ono, K., Mano, M., Sakabe, A., Miyata, A., Takahashi, K. (2014), Cross-
571 validation of open-path and closed path eddy-covariance techniques for observing methane
572 fluxes. *Boundary-Layer Meteorology*, 151(1), 95-118. doi:10.1007/s10546-013-9890-2
- 573
- 574 Iwata, H., Hirata, R., Takahashi, Y., Miyabara, Y., Itoh, M., and Iizuka, K. (2018), Partitioning
575 eddy-covariance methane fluxes from a shallow lake into diffusive and ebullitive fluxes.
576 *Boundary-Layer Meteorology*, 169(3), 413-428. doi:10.1007/s10546-018-0383-1
- 577
- 578 Jammet, M., Crill, P., Dengel, S., and Friborg, T. (2015), Large methane emissions from a
579 subarctic lake during spring thaw: mechanisms and landscape significance. *Journal of*
580 *Geophysical Research: Biogeosciences*, 120(11), 2289-2305. doi:10.1002/2015JG003137
- 581
- 582 Jammet, M., Dengel, S., Kettner, E., Parmentier, F. W., Wik, M., Crill, P., and Friborg, T.
583 (2017), Year-round CH₄ and CO₂ flux dynamics in two contrasting freshwater ecosystems of the
584 subarctic. *Biogeosciences*, 14(22), 5189-5216. doi:10.5194/bg-14-5189-2017
- 585
- 586 Jansen, J., Thornton, B. F., Jammet, M. M., Wik, M., Cortés, A., Friborg, T., MacIntyre, S., and
587 Crill, P. M. (2019), Climate-sensitive controls on large spring emissions of CH₄ and CO₂ from
588 northern lakes. *Journal of Geophysical Research: Biogeosciences*, 124(7), 2379-2399.
589 doi:10.1029/2019JG005094
- 590
- 591 Joyce, J. and Jewell, P. W. (2003), Physical controls on methane ebullition from reservoirs and
592 lake. *Environmental and Engineering Geosciences*, 9(2), 167-178. doi:10.2113/9.2.167
- 593
- 594 Kormann, R. and Meixner F. X. (2001), An analytical footprint model for non-neutral
595 stratification. *Boundary-Layer Meteorology*, 99(2), 207-224. doi:10.1023/A:1018991015119
- 596
- 597 Liikanen, A., Huttunen, J. T., Murtoniemi, T., Tanskanen, H., Väisänen, T., Silvola, J., Alm, J.,
598 and Martikainen, P. J. (2003), Spatial and seasonal variation in greenhouse gas and nutrient
599 dynamics and their interactions in the sediments of a boreal eutrophic lake. *Biogeochemistry*,
600 65(1), 83-103. doi:10.1023/A:1026070209387
- 601
- 602 Liu, L., Xu, M., Li, R., and Shao, R. (2017), Timescale dependence of environmental controls on
603 methane efflux from Poyang Hu, China. *Biogeosciences*, 14(8), 2019-2032. doi:10.5194/bg-14-
604 2019-2017
- 605
- 606 MacIntyre, S., Jonsson, A., Jansson, M., Aberg, J., Turney, D. E. and Miller, S. (2010),
607 Buoyancy flux, turbulence, and the gas transfer coefficient in a stratified lake. *Geophysical*
608 *Research Letters*, 37(24), L24604. doi:10.1029/2010GL044164
- 609

- 610 Magen, C., Lapham, L. L., Pohlman, J. W., Marshall, K., Bosman, S., Casso, M., Chanton, J. P.
611 (2014), A simple headspace equilibration method for measuring dissolved methane. *Limnology*
612 *and Oceanography: Methods*, 12(9), 637-650. doi:10.4319/lom.2014.12.637
613
- 614 Mahrt, L. (1998), Flux sampling errors for aircraft and towers. *Journal of Atmospheric and*
615 *Oceanic Technology*, 15(2), 416-429. doi:10.1175/1520-
616 0426(1998)015<0416:FSEFAA>2.0.CO;2
617
- 618 McDermitt, D., Burba, G., Xu, L., Anderson, T., Komissarov, A., Riensche, B., Schedlbauer, J,
619 Starr, G., Zona, D., Oechel, W., Oberbauer, S., and Hastings, S. (2011), A new low-power, open-
620 path instrument for measuring methane flux by eddy covariance. *Applied Physics B*, 102(2), 391-
621 405. doi:10.1007/s00340-010-4307-0
622
- 623 Park, H., Iwami, C., Watanabe, M. F., Harada, K., Okino, T., Hayashi, H. (1998), Temporal
624 variabilities of the concentrations of intra- and extracellular microcystin and toxic microcystis
625 species in a hypertrophic lake, Lake Suwa, Japan (1991-1994). *Environmental Toxicology and*
626 *Water Quality*, 13(1), 61-72. doi:10.1002/(SICI)1098-2256(1998)13:1<61::AID-
627 TOX4>3.0.CO;2-5
628
- 629 Podgrajsek, E., Sahlée, E., and Rutgersson, A. (2014), Diurnal cycle of lake methane flux.
630 *Journal of Geophysical Research: Biogeosciences*, 119(3), 236-248. doi:10.1002/2013JG002327
631
- 632 Podgrajsek, E., Sahlée, E., Bastviken, D., Natchimuthu, S., Kljun, N., Chmiel, H. E.,
633 Klemedtsson, L., and Rutgersson, A. (2016), Methane fluxes from a small boreal lake measured
634 with the eddy covariance method. *Limnology and Oceanography*, 61(S1), S41-S50.
635 doi:10.1002/lno.10245
636
- 637 Rey-Sanchez, A. C., Morin, T. H., Stefanik, K. C., Wrighton, K., and Bohrer, G. (2018),
638 Determining total emissions and environmental drivers of methane flux in a Lake Erie estuarine
639 marsh. *Ecological Engineering*, 114(15), 7-15. doi:10.1016/j.ecoleng.2017.06.042
640
- 641 Saunois, M., Bousquet, P., Poulter, B., Peregón, A., Ciais, P., Canadell, J. G., Dlugokencky, E.
642 J., Etiope, G., Bastviken, D., Houweling, S., Janssens-Maenhout, G., Tubiello, F. N., Castaldi, S.,
643 Jackson, R. B., Alexe, M., Arora, V. K., Beerling, D. J., Bergamaschi, P., Blake, D. R.,
644 Brailsford, G., Brovkin, V., Bruhwiler, L., Crevoisier, C., Crill, P., Covey, K., Curry, C.,
645 Frankenberg, C., Gedney, N., Höglund-Isaksson, L., Ishizawa, M., Ito, A., Joos, F., Kim, H.-S.,
646 Kleinen, T., Krummel, P., Lamarque, J.-F., Langenfelds, R., Locatelli, R., Machida, T.,
647 Maksyutov, S., McDonald, K. C., Marshall, J., Melton, J. R., Morino, I., Naik, V., O'Doherty, S.,
648 Parmentier, F.-J. W., Patra, P. K., Peng, C., Peng, S., Peters, G. P., Pison, I., Prigent, C., Prinn,
649 R., Ramonet, M., Riley, W. J., Saito, M., Santini, M., Schroeder, R., Simpson, I. J., Spahni, R.,
650 Steele, P., Takizawa, A., Thornton, B. F., Tian, H., Tohjima, Y., Viovy, N., Voulgarakis, A., van
651 Weele, M., van der Werf, G. R., Weiss, R., Wiedinmyer, C., Wilton, D. J., Wiltshire, A.,
652 Worthy, D., Wunch, D., Xu, X., Yoshida, Y., Zhang, B. Zhang, Z., and Zhu, Q. (2016), The
653 global methane budget 2000-2012. *Earth System Science Data*, 8(2), 697-751. doi:10.5194/essd-
654 8-697-2016
655

- 656 Schotanus P., Nieuwstadt F. T. M, and de Bruin H. A. R. (1983), Temperature measurement with
657 a sonic anemometer and its application to heat and moisture fluxes. *Boundary-Layer*
658 *Meteorology*, 26(1), 81–93. doi:10.1007/BF00164332
659
- 660 Schubert, C. J., Diem, T., and Eugster, W. (2012), Methane emissions from a small wind
661 shielded lake determined by eddy covariance, flux chambers, anchored funnels, and boundary
662 model calculations: a comparison. *Environmental Science and Technology*, 46(8), 4515-4522.
663 doi:10.1021/es203465x
664
- 665 Stepanenko, V., Mammarella, I., Ojala, A., Miettinen, H., Lykosov, V., and Veasala, T. (2016),
666 LAKE 2.0: a model for temperature, methane, carbon dioxide and oxygen dynamics in lakes.
667 *Geoscientific Model Development*, 9(5), 1977-2006. doi:10.5194/gmd-9-1977-2016
668
- 669 Subin, Z. M., Murphy, L. N., Li, F., Bonfils, C., and Riley, W. J. (2012), Boreal lakes moderate
670 seasonal and diurnal temperature variation and perturb atmospheric circulation: analysis in the
671 Community Earth System Model 1 (CESM1). *Tellus A*, 64(1), 15639.
672 doi:10.3402/tellusa.v64i0.15639
673
- 674 Tedford, E. W., MacIntyre, S., Miller, S. D., and Czikowsky, M. J. (2014), Similarity scaling of
675 turbulence in a temperate lake during fall cooling. *Journal of Geophysical Research: Oceans*,
676 119(8), 4689-4713. doi:10.1002/2014JC010135
677
- 678 Thebrath, B., Rothfuss, F., Whitar, M. J., and Conrad, R. (1993), Methane production in littoral
679 sediment of Lake Constance. *FEMS Microbiology Ecology*, 11(3-4), 279-289.
680 doi:10.1111/j.1574-6968.1993.tb05819.x
681
- 682 Tokida, T., Miyazaki, T., and Mizoguchi, M., Nagata, O., Takakai, F., Kagemoto, A., and
683 Hatano, R., (2007), Falling atmospheric pressure as a trigger for methane ebullition from
684 peatland. *Global Biogeochemical Cycles*, 21(2), GB2003. doi:10.1029/2006GB002790
685
- 686 Utsumi, M., Nojiri, Y., Nakamura, T., Nozawa, T., Otsuki, A., and Seki, H. (1998), Oxidation of
687 dissolved methane in a eutrophic, shallow lake: Lake Kasumigaura, Japan. *Limnology and*
688 *Oceanography*, 1998, 43(3), 471–480. doi:10.4319/lo.1998.43.3.0471
689
- 690 van de Boer, A., Moene, A. F., Graf, A., Schüttemeyer, D., and Simmer, C. (2014), Detection of
691 entrainment influences on surface-layer measurements and extension of Monin-Obukov
692 similarity theory. *Boundary-Layer Meteorology*, 152(1), 19-44. doi:10.1007/s10546-014-9920-8
693
- 694 Vickers, D. and Mahrt, L. (1997), Quality control and flux sampling problems for tower and
695 aircraft data. *Journal of Atmospheric and Oceanic Technology*, 14(3), 512-526.
696 doi:10.1175/1520-0426(1997)014<0512:QCAFSP>2.0.CO;2
697
- 698 Wanninkhof, R., Asher, W. E., Ho, D. T., Sweeney, C., and McGillis, W. R. (2009), Advanced
699 in quantifying air-sea gas exchange and environmental forcing. *Annual Review of Marine*
700 *Science*, 1, 213-244. doi:10.1146/annurev.marine.010908.163742
701

702 Webb, E. K., Pearman, G. L. and Leuning, R. (1980), Correction of flux measurements for
703 density effects due to heat and water vapor transfer. *Quarterly Journal of the Royal*
704 *Meteorological Society*, 106, 85-100. doi:10.1002/qj.49710644707

705
706 Wik, M., Patrick, M. C., Varner, R. K., and Bastviken, D. (2013), Multiyear measurements of
707 ebullitive methane flux from three subarctic lakes. *Journal of Geophysical Research:*
708 *Biogeosciences*, 118(3): 1307-1321. doi:10.1002/jgrg.20103

709